Journal of Inflammation Research

Dovepress
Taylor & Francis Group

Open Access Full Text Article

ORIGINAL RESEARCH

IL7-IL7R Interaction Mediates Fibroblast-Driven Macrophage-to-Osteoclast Differentiation in Periodontitis

Pengjie Huang[1,*], Li Gao[1,*], Jiezhong Guan[1], Yijiao Li[1], Yibing Jia[1], Zixiang Zeng[1], Yurun Chen[1], Linge Wang[2], Weichang Li[1], Yan Wang[1], Bo Yang[1]

[1]Hospital of Stomatology, Guanghua School of Stomatology, Sun Yat-Sen University, Guangdong Provincial Key Laboratory of Stomatology, Guangzhou, People's Republic of China; [2]South China Advanced Institute for Soft Matter Science and Technology, School of Molecular Science and Engineering, Guangdong Provincial Key Laboratory of Functional and Intelligent Hybrid Materials and Devices, South China University of Technology, Guangzhou, People's Republic of China

*These authors contributed equally to this work

Correspondence: Yan Wang; Bo Yang, Email wangyan9@mail.sysu.edu.cn; yangb86@mail.sysu.edu.cn

Aim: To identify osteoclastogenic macrophage subsets and their regulatory mechanisms in periodontitis.

Methods: We integrated single-cell RNA sequencing datasets from human and murine periodontitis to construct a comprehensive macrophage and monocyte atlas. Employing functional enrichment, cell-cell communication, pseudotime, transcription factor, and machine learning analyses, we characterized and selected the specific macrophage subset involved in cell interactions. In vitro and in vivo experiments, including enzyme-linked immunosorbent assay, TRAP staining, micro-CT, qPCR, flow cytometry, and immunofluorescence staining, were performed to dissect the osteoclastogenic potential of specific macrophage subsets and to identify the key pathways.

Results: We discovered that the IL7R$^+$ macrophage subset possesses significant osteoclast differentiation potential. Our findings indicate that the IL7/IL7R signaling axis facilitates osteoclast differentiation. Genes highly expressed in IL7R$^+$ macrophages were identified as strong predictors for periodontitis by machine learning models. In vivo and in vitro experimental validation confirmed an increase in IL7R$^+$ macrophages, along with their enhanced osteoclastogenic capacity. confirmed an increase in IL7R$^+$ macrophages, along with their osteoclastogenic capacity. The inhibition of the IL7/IL7R signaling pathway was found to mitigate periodontitis progression by impeding osteoclast differentiation. Furthermore, fibroblasts were found to secret IL7 interacting with IL7 receptors on macrophages.

Conclusion: Our study identifies IL7R$^+$ macrophages as potential osteoclast precursors in periodontitis. We demonstrate that the IL7/IL7R signaling pathway is a critical driver of osteoclast differentiation. Moreover, targeting IL7R is a potential therapeutic strategy to curb periodontitis bone resorption.

Keywords: periodontitis, single-cell sequencing, osteoclast differentiation, macrophage

Introduction

Periodontitis (PD) represents a prevalent condition affecting 61.9% of the global population, characterized by chronic inflammation caused by microbial infection in the subgingival dental biofilm.[1,2] In the periodontal inflammation microenvironment, immune cells such as macrophages, T cells, B cells, and dendritic cells are activated by virulence factors like lipopolysaccharides (LPS), contributing to the production of pro-inflammatory cytokines and amplifying the inflammatory response.[3] This chronic inflammation disrupts the balance between osteoclast-mediated bone resorption and osteoblast-mediated bone formation, resulting in alveolar bone loss.[4]

The cornerstone of PD management—mechanical scaling and root planing (SRP) combined with systemic antibiotics—aims to reduce microbial load and inflammation.[5] However, SRP often fails to completely eradicate dental calculus and

Received: 13 March 2025
Accepted: 3 May 2025
Published: 11 May 2025

Graphical Abstract

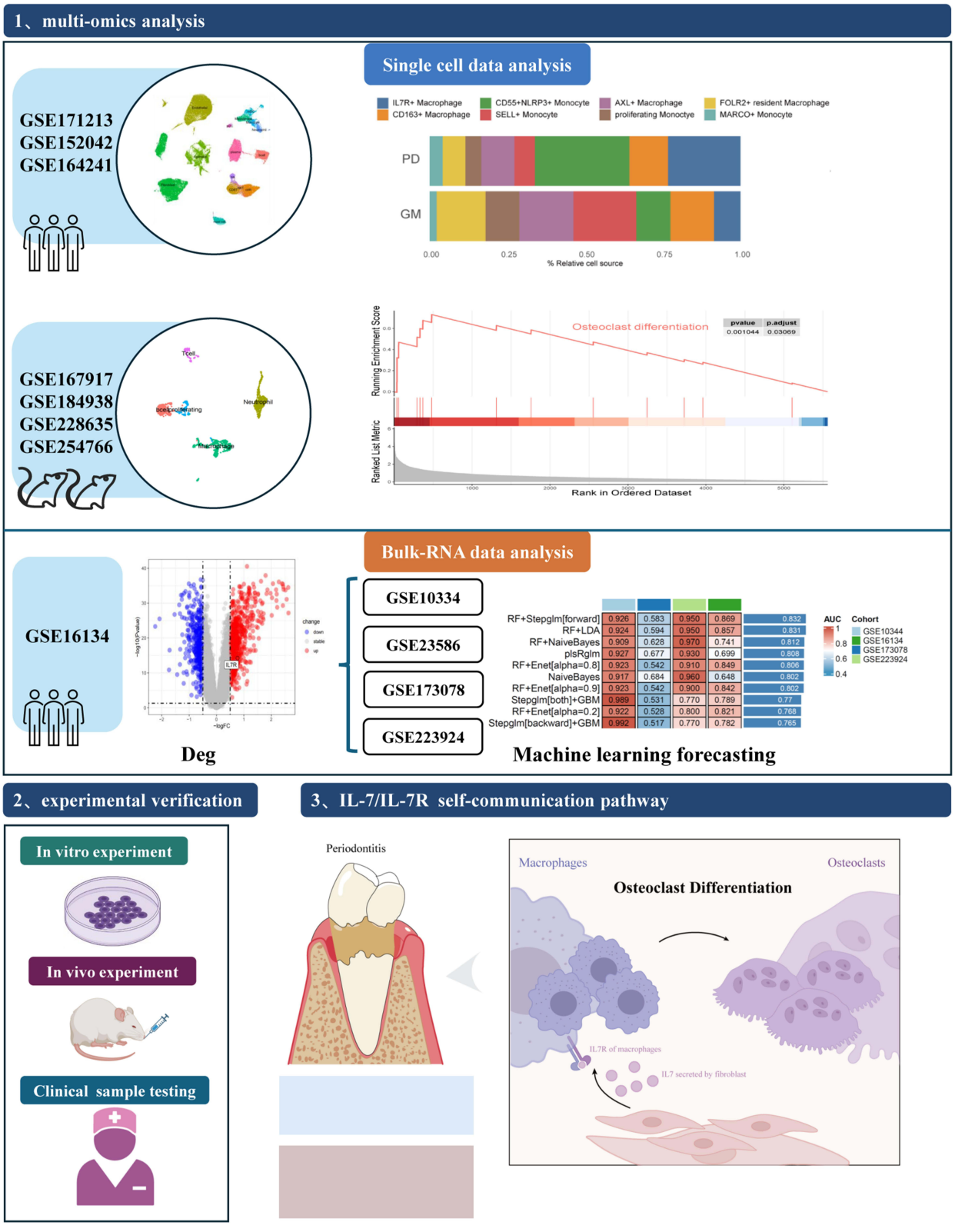

endotoxins embedded in deep periodontal pockets, while nonspecific antibiotic distribution results in subtherapeutic concentrations at lesion sites.[2,6] These limitations perpetuate a pro-inflammatory microenvironment, wherein residual pathogens and their byproducts (eg, LPS) sustain macrophage activation. Sustained cytokine release further amplifies RANKL/OPG axis dysregulation, skewing bone homeostasis toward excessive osteoclastogenesis and irreversible alveolar bone loss.[7]

Macrophages are important in the regulation of bone homeostasis, serving as pivotal mediators of both inflammatory responses and bone remodeling.[8] In response to microbial challenges such as LPS, macrophages undergo activation and polarization, which critically influence osteoclast differentiation.[9] In periodontitis, there is a notable shift in macrophage polarization: during the early stages, M1 macrophages dominate, releasing pro-inflammatory cytokines (eg, TNF-α and IL-1β) that not only intensify the inflammatory cascade but also indirectly promote osteoclastogenesis.[10] In contrast, M2 macrophages—typically associated with anti-inflammatory and tissue repair functions—are inadequately represented, failing to counterbalance the excessive inflammatory signals. This changed M1/M2 ratio compromises the resolution of inflammation and further destabilizes the equilibrium between bone formation and resorption.[11]

Recent studies suggest that fibroblasts, the primary stromal cells in periodontal tissues, may play a critical role in regulating macrophage-driven osteoclastogenesis through paracrine signaling.[12] Under inflammatory conditions, gingival fibroblasts secrete interleukin-7 (IL-7) in response to microbial components (eg, LPS).[13–15] While IL-7 is classically associated with lymphocyte regulation, its role in osteoclastogenesis remains controversial: some studies indicate IL-7 suppresses osteoclast differentiation via T cell modulation, whereas others propose direct pro-osteoclastic effects through IL-7 receptor (IL-7R) signaling in myeloid cells.[16] Importantly, the contribution of fibroblast-derived IL-7 to macrophage osteoclastogenic programming in periodontitis remains unexplored. This knowledge gap is critical because fibroblasts and macrophages colocalize in inflammatory bone resorption niches, suggesting spatially restricted IL-7/IL-7R crosstalk may synergize with RANKL to amplify osteoclastogenesis—a hypothesis yet to be tested.

Single-cell RNA sequencing (scRNA-seq) has emerged as a transformative tool for deconvoluting cellular heterogeneity and uncovering rare pathogenic subsets in complex inflammatory diseases.[17] Unlike bulk RNA-seq, which masks cell-type-specific signatures, scRNA-seq enables high-resolution mapping of transcriptional states, including transitional phenotypes and niche-specific cellular crosstalk.[18] Although recent scRNA-seq studies in PD have cataloged gingival immune populations, two limitations hinder progress. Fragmented datasets from individual studies lack cross-cohort integration to identify conserved disease-associated changes. In addition, macrophage subpopulations are crudely annotated without functional stratification (eg, pro-osteoclastic vs immunoregulatory subsets). Integrative analysis of multi-source scRNA-seq data, coupled with trajectory inference and cell-cell communication modeling, could resolve these limitations and pinpoint macrophage subsets driving osteoimmune dysregulation.[19,20]

In our study, we utilized single-cell RNA sequencing (scRNA-seq) datasets and bulk RNA-seq to dissect gingival tissue cellular heterogeneity in both healthy and periodontitis gingival. We aimed to explore whether a disease-specific expansion of $IL7R^{+}$ macrophages occurs within periodontal lesions and to assess the potential role of fibroblast-derived IL7 in modulating osteoclastogenesis. In addition, the study examines the impact of pharmacological IL7R blockade and in vitro co-culture models on osteoclast differentiation, to elucidate the mechanisms underlying pathological bone resorption and evaluating the therapeutic potential of targeting the IL7/IL7R signaling pathway.

Methods and Materials

Data Acquisition

The metadata of the single-cell atlas was described by the provider. The human single-cell data was obtained from GSE164241, GSE171213, and GSE152042. The mice single-cell data was obtained from GSE167917, GSE184938, GSE228635, and GSE254766. The bulk RNA data was obtained from GSE10334, GSE16134, GSE23586, GSE173078, and GSE223924.

Analysis of Single-Cell Data

The data analysis was primarily performed by the Seurat package (version 5.0.1). DecontX (version 0.99.3) was utilized to remove RNA contamination, setting the contamination parameter to less than 0.2. DoubletFinder (2.0.3) was employed to remove the double cell, provisionally. After NormalizeData, FindVariableFeatures, and ScalaData, the layers of data were integrated by harmony. Subsequently, the cluster was found by FindClusters, with the resolution setting to 5 to eliminate the double cell cluster. The $IL7R^{+}$ macrophages were defined based on a marker-based approach utilizing single-cell sub-clustering. Specifically, we identified these cells by examining the expression levels of established markers, including IL7R, which reliably distinguishes this subpopulation. The clustering was performed using standard single-cell RNA sequencing analysis techniques, ensuring that the cells assigned to the $IL7R^{+}$ subgroup exhibit a distinct and biologically relevant expression profile. The proportions of cell clusters in each sample were calculated, and differential analysis was performed using the Wilcoxon rank-sum test.

Finding Differentially Expressed Genes

We employed the FindAllMarkers function, with the setting min. pct = 0.1, logfc. threshold = 0.25, and p_val_adj < 0.05, to identify significantly differentially expressed genes. These genes were then assessed and annotated to distinguish between subgroups based on existing biological knowledge.

Functional Analysis

Functional analysis was conducted to identify differentially expressed genes (DEGs) across clusters using the FindAllMarkers function in Seurat. These genes were subsequently analyzed through KEGG and GSEA pathway enrichment. Additionally, the AUCell (version 1.22.0) package, inputting the GOBP_OSTEOCLAST_DIFFERENTIATION gene signature, was utilized to pinpoint active gene sets linked to specific pathways.

Cell-Cell Interaction Analysis

Cell-cell interaction analysis was performed using CellChat (version 1.6.1) to evaluate the communication patterns among various cell types.

Trajectory Analysis

Trajectory analysis to picture differentiation trajectory among macrophage subtypes was executed by Monocle3 (version 1.3.5). CytoTRACE (version 0.3.3) was employed to predict the initiation point.

Transcript Factor Analysis

Transcript factor analysis was performed by pyscenic (version 0.12.1) on human periodontitis macrophage subclusters. This process involved identifying regulons based on the co-expression of transcription factors and their target genes, as sourced from the RCisTarget database.

Preprocessing of Bulk Transcriptome Data

The differentially expressed genes of geo data were analyzed by limma package (version 3.56.2). The threshold of differentially expressed genes was set as logFC_t > 0.5 and P. Value_t < 0.05.

Deconvolution

CIBERSORTx was employed to estimate the relative abundance of each macrophage subtype. The bulk transcriptome was the GSE10334. The reference single-cell dataset included 8 macrophage and monocyte cell types.

Machine Learning for Prediction Models of Periodontitis

The selection of key genes for the machine learning models was performed by applying the "COSG" function to the $IL7R^+$ macrophage subpopulation. This analysis systematically identified genes with significantly higher expression in this subpopulation compared to others. From these, the top 10 genes exhibiting the most pronounced differential expression and specificity for $IL7R^+$ macrophages were chosen as features for the machine learning models, providing a predictive framework based on biologically relevant markers. Subsequently, we set the data GSE10334 and GSE173078 as the training set and the data GSE16134 and GSE223924 as the testing set.

Cell Culture

The THP-1 human monocyte cell line (CL-0233, Procell, China) was propagated in the RPMI 1640 medium. The THP-1 was seeded into 12 well plates at a density of 1*105/mL. 100ng/mL Phorbol 12-myristate 13-acetate (PMA, MCE, US) was added for 48h to induce M0 macrophages. Macrophages derived from THP-1 were subjected to medium changes every three days, with the addition of 50ng/mL RANKL (MCE, US) and 30ng/mL M-CSF(MCE) to induce osteoclast differentiation for 14 days. For the PD group, macrophages were treated with 100ng/mL Pg.LPS (invivogen, France) during the initial 48 hours in osteoclast differentiation. For the ANTI-IL7R group, 1μg/mL Lusvertikimab (MCE) and 100ng/mL Pg.LPS were added during the first 48 hours of osteoclast differentiation. The HGF-1 human gingival fibroblast cell line (CP-0240, Procell, China) was cultured in the DMEM medium. After seeding, fibroblasts were treated with 100ng/mL Pg.LPS for 48 hours.

Animals

C57BL/6 male mice aged 5 to 8 weeks were obtained from the Laboratory Animal Center, Sun Yat-sen University East Campus. The mice were housed in a sterile, pathogen-free environment within a regulated clean facility at the Experimental Medicine Institute. All experimental procedures followed the ARRIVE Guidelines for Animal Research: In vivo Experimental Reports and adhered to the ethical principles and requirements specified in the relevant laws and regulations, including the Sun Yat-sen University Experimental Animal Center's Animal Welfare and Ethics Management Regulations and the IACUC Charter. The study protocol was reviewed and approved by the Committee for Animal Welfare and Use at Sun Yat-sen University (Approval No. 2023002257) on January 17, 2024.

Ligature-Induced Periodontitis Model

Mice received administration of Sodium Pentobarbital at a 0.3% concentration (equivalent to 3 mg/mL) in a dose of 50 mg per kilogram of body weight. Subsequently, a ligature (5–0 silk) was positioned encircling the right maxillary second molar from the initial day up to the 14th day. For the healthy group, anesthesia was administered without the application of ligature. For the ANTI-IL7R group, 5μg of IL7R blocking antibody (BE0065, InVivoMAb, US) was injected into the gingiva every three days following the silk ligature placement. Mice were euthanized after 14 days.

Immunofluorescence (IF) Staining

The IL7R antibody (1:100 Santa Cruz Biotechnology, US), TRAP antibody (1:100 abcam, UK) were incubated for 12h at 4°C. Secondary antibodies conjugated with FITC or TITRC were incubated at room temperature for 1 hour, followed by mounting with an anti-fade mounting medium containing DAPI.

TRAP Staining

The TRAP staining kit (Solarbio, China) was used according to the instructions provided for cells and tissues. TRAP staining occurred at 37°C in darkness for 60 minutes, followed by nuclear staining using hematoxylin for 2 minutes. The stained sections were scanned with a slide scanner (3DHISTECH panoramic MIDI II).

Enzyme-Linked Immunosorbent Assay (ELISA)

Clinical periodontal tissues were pulverized using RIPA lysis buffer and subjected to centrifugation (13,000g, 4°C, for 20 minutes). Macrophage culture supernatant of each group was collected after 48 hours' stimulation with P.g LPS. IL-7 in the tissues and cell culture supernatant were detected with human IL-7, human IL-6, human IL-8, and mice IL-7 ELISA kit (MEIMIAN, Jiangsu, China) according to the manufacturer's instructions.

Flow Cytometry

The cell was collected and isolated. A flow cytometer (angilent novocyte) was used for detection. The antibodies for incubating included FITC anti-human CD68 (1:200 biolegend, US), PE anti-human CD127(IL7R) (1:200 biolegend, US), Isotype control (1:200 biolegend, US). The data were analyzed with Flowjo (version 10.6.2).

Cell Co-Culture

For the co-culture experiment, the supernatant from HGF-1 cells, with or without co-culture with Pg-LPS, was collected and subsequently added to THP-1 cells. After LPS stimulation, the medium was replaced with serum-free culture medium, and the supernatant collected 1-day post-treatment was used to eliminate protein and serum interference. In the antibody blockade group, both the supernatant and IL-7 neutralizing antibody (Invitrogen, USA) were introduced to inhibit cell communication.

RNA Extraction and qRT-PCR

Briefly, total RNA was isolated from cells, along with mice periodontal tissue, utilizing TRIzol (Invitrogen, US), according to the manufacturer's instructions. Subsequently, a system containing 1000 ng was prepared for reverse transcription into cDNA. The levels of mRNA expression were quantified utilizing SYBR Green PCR Master Mix (YEASEN, CHINA) along with the 7900HT sequence detection system from Applied Biosystems. Furthermore, the relative expression level of mRNA was determined through the 2^(-ΔΔCt) technique and standardized against glyceraldehyde 3-phosphate dehydrogenase (GAPDH). The information of the primers is provided in Supplementary Table 1.

μCT

Maxillary bone samples were scanned with a micro-CT scanner (Scano Micro-CT, μCT50, Switzerland) at a voxel resolution of 10μm with an energy of 70kV, and 200mA. Three-dimensional microstructural imagery was regenerated.

Patient Samples

This study was conducted in accordance with the Declaration of Helsinki. The periodontal tissue attached to the extracted tooth was collected from healthy and periodontitis patients after tooth extraction. Samples were collected with the participants' informed consent and the collecting scheme was agreed by the medical ethics committee of the Hospital of Stomatology Sun Yat-sen University (KQEC-2024-43-01). The standard for periodontitis was probing depth larger than 4mm and clinical attachment loss larger than 2mm, corresponding to stage II (moderate) or stage III (severe) periodontitis. For the GM group, the probing depth was smaller than 4mm, and the clinical attachment was smaller than 2mm. We collected 5 samples for each group. The clinical data of the patient's samples is shown in Supplementary Table 2.

Statistics

We conducted all data analyses using GraphPad Prism 9.3.0 (GraphPad, Bethesda, MD). Data were presented as mean ± standard deviations. To assess differences among multiple groups, we applied one-way ANOVA with Tukey's multiple comparisons test. For comparisons between the two groups, we employed an unpaired, two-tailed Student's *t*-test.

Results

Identification of IL7R$^+$ Macrophage as a Periodontitis-Associated Subset

To create a comprehensive single-cell transcriptome atlas of the gingival microenvironment, we obtained the scRNA-seq data from three published single-cell datasets (GSE171213, GSE164241, GSE152042). After quality control, we manually removed double cells based on their top expressed marker found by Findallmarkers. Subsequently, we manually annotated clusters by characteristic expression genes of each cell type and identified 4 main cell types -immune, endothelial, fibroblast, and epithelial-where only immune cells exhibited significant differences between periodontitis and normal groups (Figure S1A and S1E). Additionally, we further annotated immune cell subtypes, including myeloid cells, to refine our analysis (Figure S1B and S1C). We finally acquired 15 clusters of cells, including B cell, CD4 T cell, endothelial cell, epithelial cell, fibroblast, macrophage, mast cell, mDC, monocyte, neutrophil, NK, NKT, pDC, and plasma (Figure 1A). Among these subclusters, macrophages, plasma, and B cells had markedly increased in periodontitis (Figure S1F). Furthermore, differentially expressed genes (DEG) analysis was carried out to assess the gene expression in clusters, and the dot plot demonstrated the specifically expressed genes of different cell types, which are consistent with classical, well-established markers (Figure S1D). Based on the increased proportion and pivotal roles of macrophages and monocytes in inflammation as well as osteoclast differentiation in periodontitis, we selected these cells for further study.[20]

Eight subsets were characterized in macrophages and monocytes, including IL7R$^+$ macrophages, CD163$^+$ macrophages, CD55$^+$NLRP3$^+$ monocytes, SELL$^+$ monocytes, AXL$^+$ macrophages, proliferating monocytes, FOLR2$^+$ resident macrophage and MARCO$^+$ monocyte (Figure 1B). These subsets were manually annotated by characteristic expression genes (IL7R, CD163, CD55, NLRP3, SELL, AXL, FOLR2, and MARCO) (Figure 1C). Contrary, we found that other clusters showed low expression of the osteoclast-related gene. IL7R is thought to play a key role in V(D)J recombination during lymphocyte development.[21] However, based on our findings, we hypothesize that IL7R in macrophages is associated with osteoclast differentiation in periodontitis. In addition, the number of IL7R$^+$ macrophages was proved higher in PD than in normal periodontal tissue (Figure 1D). DEG analysis demonstrated the validity and credibility of clusters through feature plots (Figure 1E). Validated by vlnplot, we quantified the average expression of CD163, MMP9, ACP5, TNFRSF11A, IL7R, and CTSK. These osteoclasts' functional markers had elevated level expression in IL7R$^+$ macrophages (Figure S1G). These results together indicated the IL7R$^+$ macrophage subcluster as a periodontitis-associated subset.

IL-7R$^+$ Macrophages Differentiate Into Osteoclasts Through Single-Cell Analysis

We measured the Euclidean distance between all macrophage and monocyte subtypes (Figure 2A). The results indicated significant differences between monocytes and macrophages. To investigate the cell trajectory of macrophages and identify dynamic genes in cellular differentiation, we performed pseudotime analysis by Monocle3. The starting point for cell trajectory analysis is determined by CytoTRACE (Figure 2B). IL7R$^+$ macrophages are terminally differentiated cells and may originate from FOLR2$^+$ resident macrophages (Figure 2C). The expression of IL7R and TNFRSF11A exhibited significantly upregulated across pseudotemporal trajectory, suggesting their temporal involvement in differentiation (Figure 2D and E). KEGG enrichment analysis and GSEA analysis were employed to identify the properties of each cluster, revealing enrichment of the osteoclast differentiation pathway in IL7R$^+$ macrophages (Figure 2F and G). To further evaluate the osteoclast differentiation capacity, we conducted AUC scoring based on the geneset of the osteoclast differentiation pathway. Clustered distribution and violin plots illustrating the AUC scores were presented, demonstrating that among all macrophage subsets, IL7R$^+$ macrophages had the highest osteoclast differentiation activity AUC score (Figure 2H). Based on these findings, we believe IL7R$^+$ macrophages exhibit osteolytic activity and possess the potential for osteoclast differentiation, leading to bone absorption in periodontitis.

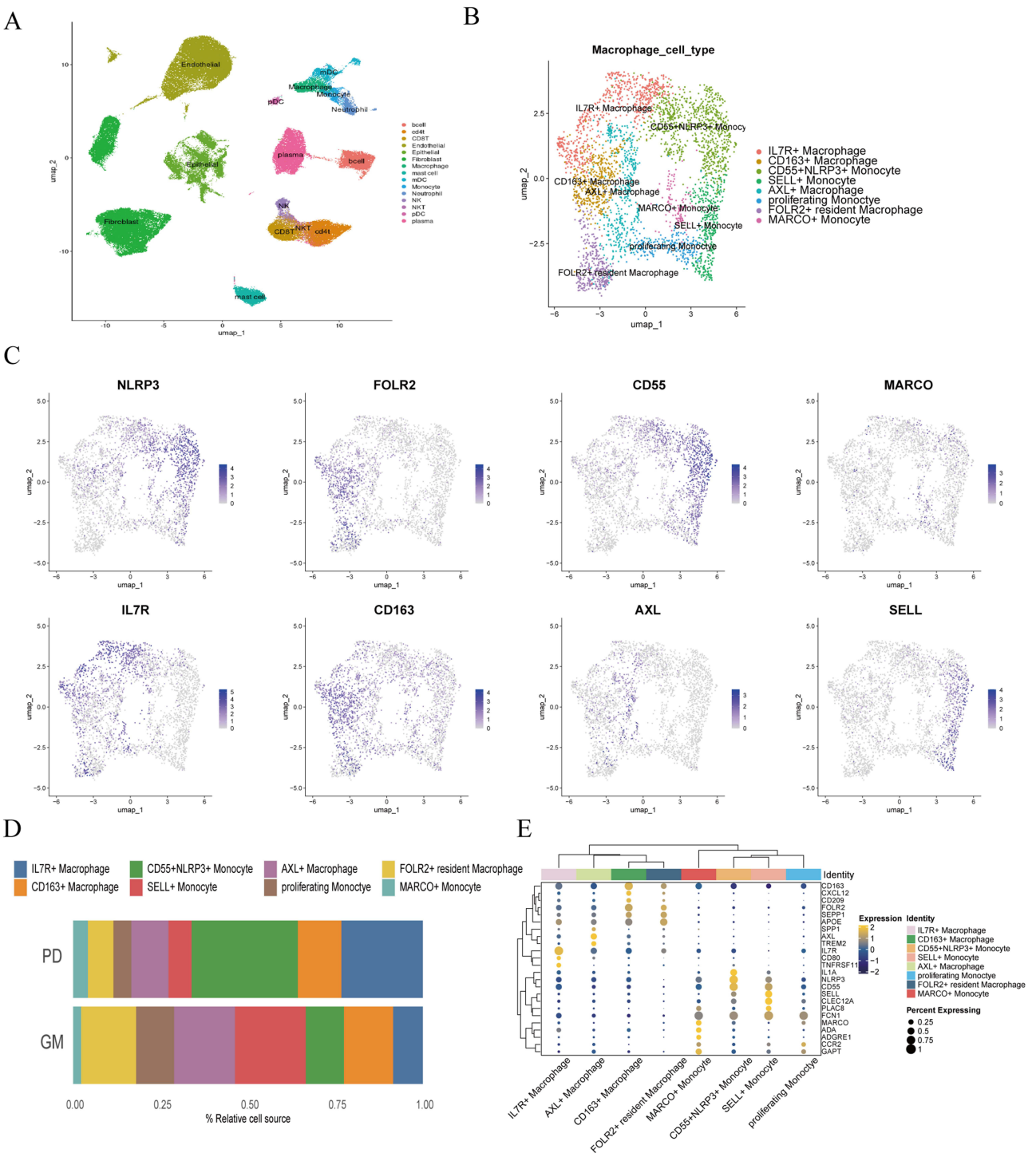

Figure 1 Identification of IL-7R^{+} macrophage as a periodontitis-associated subset. (**A**) UMAP representation of major cell types identified by scRNA seq after removal of the double cell. (n=200,000 cells) (**B**) UMAP plot of macrophage and monocyte cell types colored by subgroup clusters. (**C**) UMAP representation of the expression of marker genes of each cell type detected in this study. Blue represents high expression; gray represents low expression. (**D**) Bar graph depicting the proportion of each cell type in health (GM) and periodontitis (PD). (**E**) Dot plot revealing the gene expression levels of marker genes in each macrophage and monocyte cluster. Yellow represents high expression; blue represents low expression. The size of the circle represents the percentage of cells that express the indicated genes.

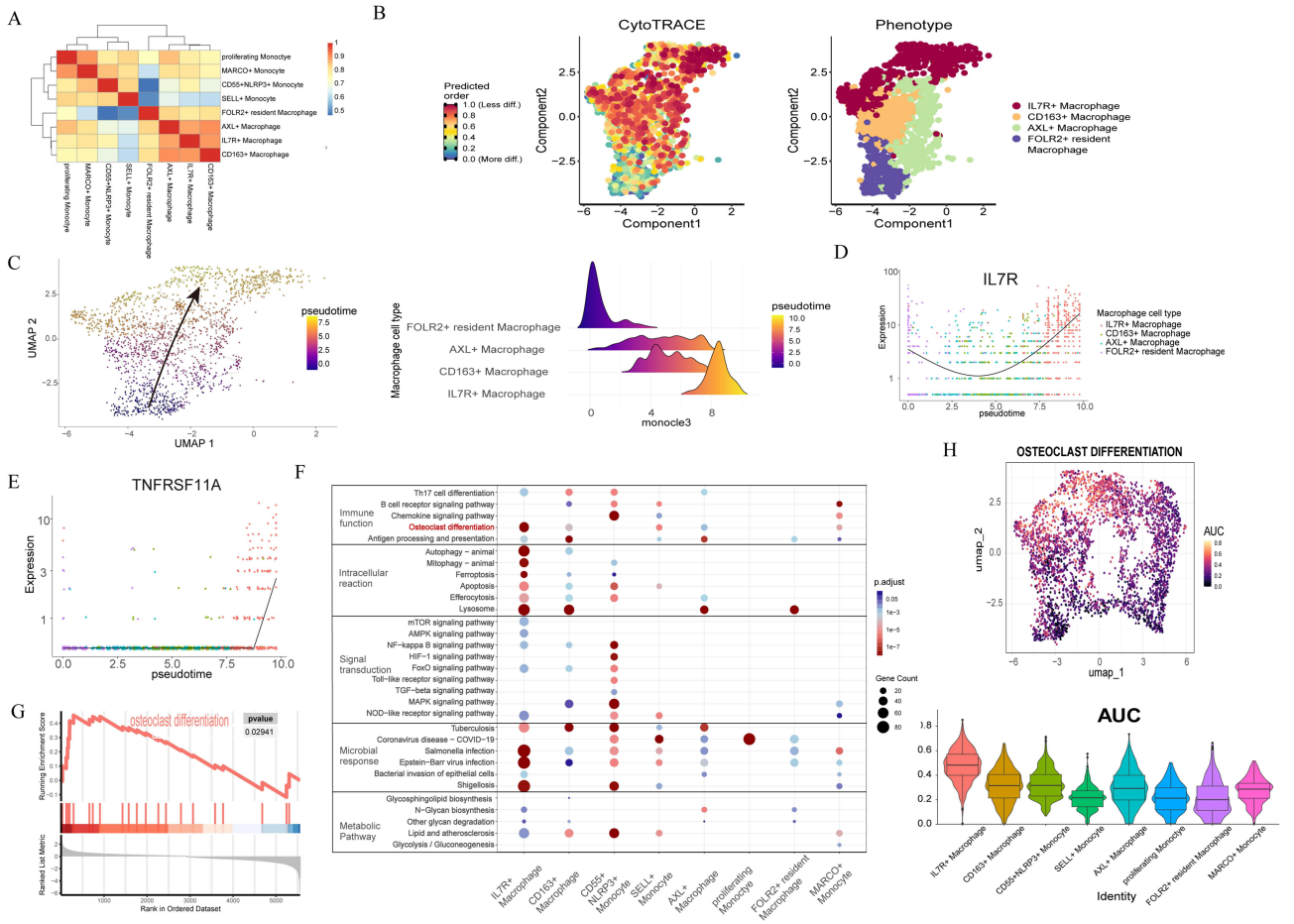

Figure 2 IL-7R$^+$ macrophages differentiate into osteoclasts through single-cell analysis. (**A**) Heatmap showing the Euclidean distances among the macrophage and monocyte subtypes. The color is the representation of communication intensity. (**B**) Pseudotime of macrophage performed by cytotrace. The colors from blue to yellow represent the order of pseudotime. (**C**) Developmental trajectory for macrophage inferred by Monocle3 and the ridgeline plot showing the IL-7R$^+$ macrophage differentiation trajectory. The colors from blue to yellow represent the order of pseudotime. (**D**) Pseudotime plot illustrating expression of IL-7R over pseudotime. (**E**) The expression changes of TNFRSF11A along the pseudotime trajectory. Red represents low p value. Blue represents high p value. The size of the points represents the number of upregulated genes in the pathway. (**F**) KEGG pathway enrichment analysis bubble chart. (**G**) GSEA analysis of osteoclast differentiation in IL7R+ macrophage. (**H**) Osteoclast differentiation activity AUC score cluster distributions and violin plot displaying the AUC score of macrophage subtypes. The dot color represents the AUC score.

The RNA Bulk Data of Periodontitis Verifies the IL7R$^+$ Macrophages as the Periodontitis Specialized Clusters

To further confirm the function of IL7R$^+$ macrophages in periodontitis, we acquired GSE16134 dataset for analysis. DEG analysis revealed the high expression of IL7R in periodontitis (Figure 3A). We constructed a machine-learning model for disease prediction based on the high-expression genes identified in the IL7R$^+$ subset (Figure 3B). In the deconvolution analysis, we utilized CIBERSORTx to evaluate the proportion of IL7R$^+$ macrophages, using single-cell data from monocytes and macrophages for annotation. This approach validated the significant upregulation of the IL7R$^+$ macrophage subset in periodontitis. (Figure 3C). To expand the sample size for learning, we incorporated bulk RNA data of periodontitis and normal tissues from 5 datasets to construct a machine learning framework. The algorithm combining Random Forest and Stepglm(forward) demonstrated robust predictive performance, and the gene expressions selected from this model were all markedly upregulated in periodontitis (Figure 3D).

IL-7R$^+$ Macrophages Exhibit Osteoclastic Characteristics Under in vitro Periodontitis-Stimulated Condition

To evaluate the osteoclastogenic potential of IL7R$^+$ macrophages, we utilized THP-1 cells and induced their differentiation into M0 macrophages. Subsequently, the cells were treated to induce osteoclast differentiation, and the PD group was added with LPS

https://doi.org/10.2147/JIR.S524284

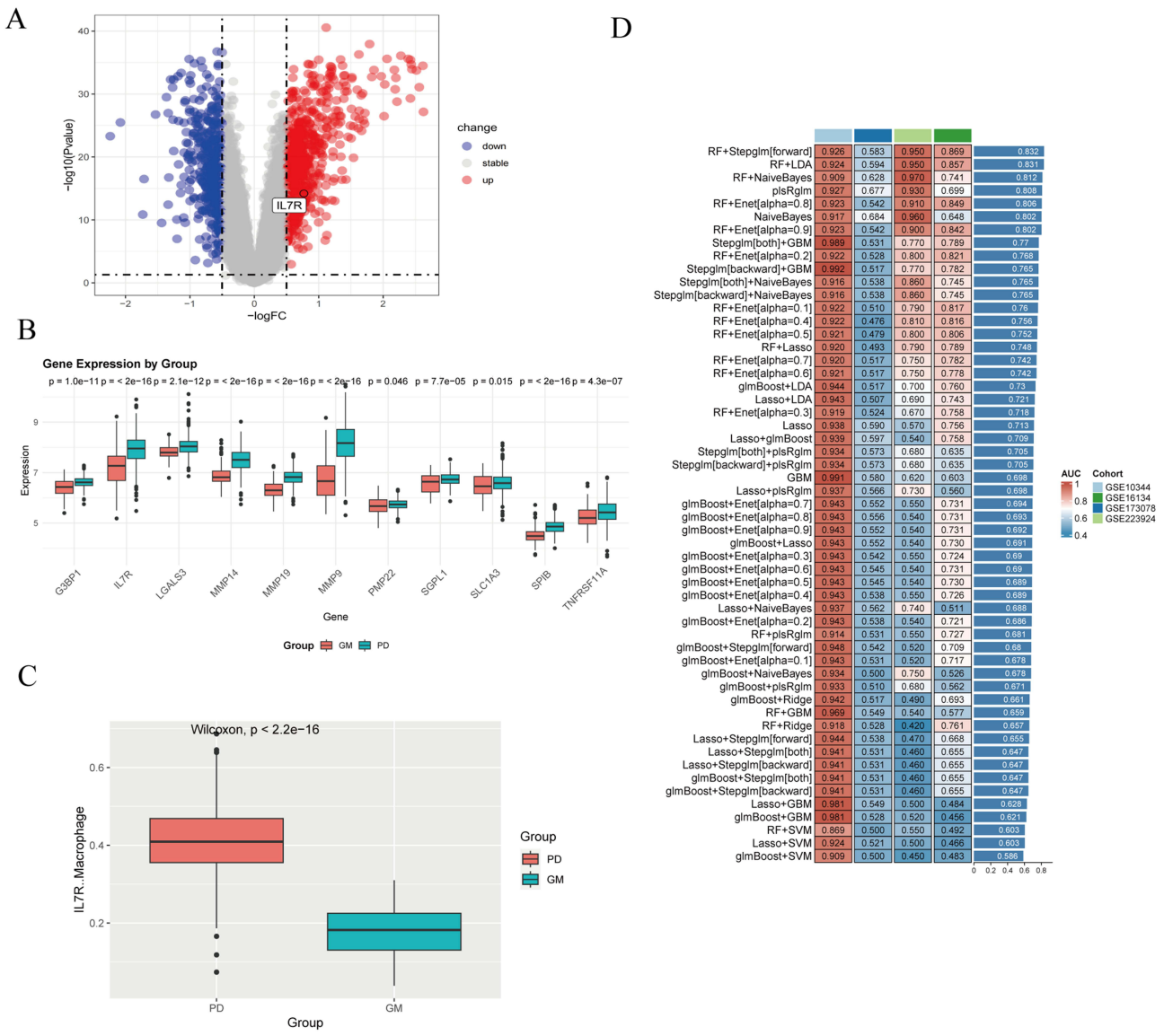

Figure 3 The RNA bulk data of periodontitis verifies the IL7R$^+$ Macrophages as the periodontitis specialized clusters. (**A**) Volcano plot of differential expression genes, with IL7R highlighted in red. (**B**) Box plot of gene expression used for machine learning, with p-values derived from the Wilcoxon rank-sum test. (**C**) The proportion of IL7R$^+$ macrophages subcluster in macrophages and monocytes evaluated by CibersortX. (**D**) Predictive performance of various machine learning algorithms for periodontitis across different cohorts.

from Porphyromonas gingivalis, while the Anti-IL7R group was treated with IL7R blocking antibody. TRAP staining revealed a significant increase in the proportion of TRAP$^+$ cells in the PD group compared to the GM group. Notably, the addition of the IL7R antibody prevented the formation of multinuclear osteoclasts (Figure 4A and C). Immunofluorescence revealed a higher abundance of TRAP$^+$IL7R$^+$ macrophages in the PD group compared to both the gingival health (GM) and Anti-IL7R groups, uncovering the enhanced osteoclastogenic potential of IL7R$^+$ macrophages (Figure 4A and B). We corroborated these findings by revealing elevated expression levels of IL7R, RANK, CTSK, and MMP9 in the PD group (Figure 4D). To more accurately investigate the quantity of IL7R$^+$ cells, we employed flow cytometry to measure the number of IL7R+ macrophages following LPS stimulation. The results indicated that the PD group exhibited a higher number of IL7R$^+$ macrophages (Figure 4E). Additionally, we utilized flow sorting technology to isolate IL7R$^+$ and IL7R$^-$ macrophages. After one week of culture, TRAP staining was performed on the sorted cells (Figure 4F). The results showed that IL7R$^+$ macrophages significantly differentiated into osteoclasts, whereas IL7R- macrophages did not differentiate into osteoclasts. We validated these results by demonstrating increased expression of IL7R, RANK, CTSK, and MMP9 in IL7R$^+$ macrophages (Figure 4G). In summary, we validated that the

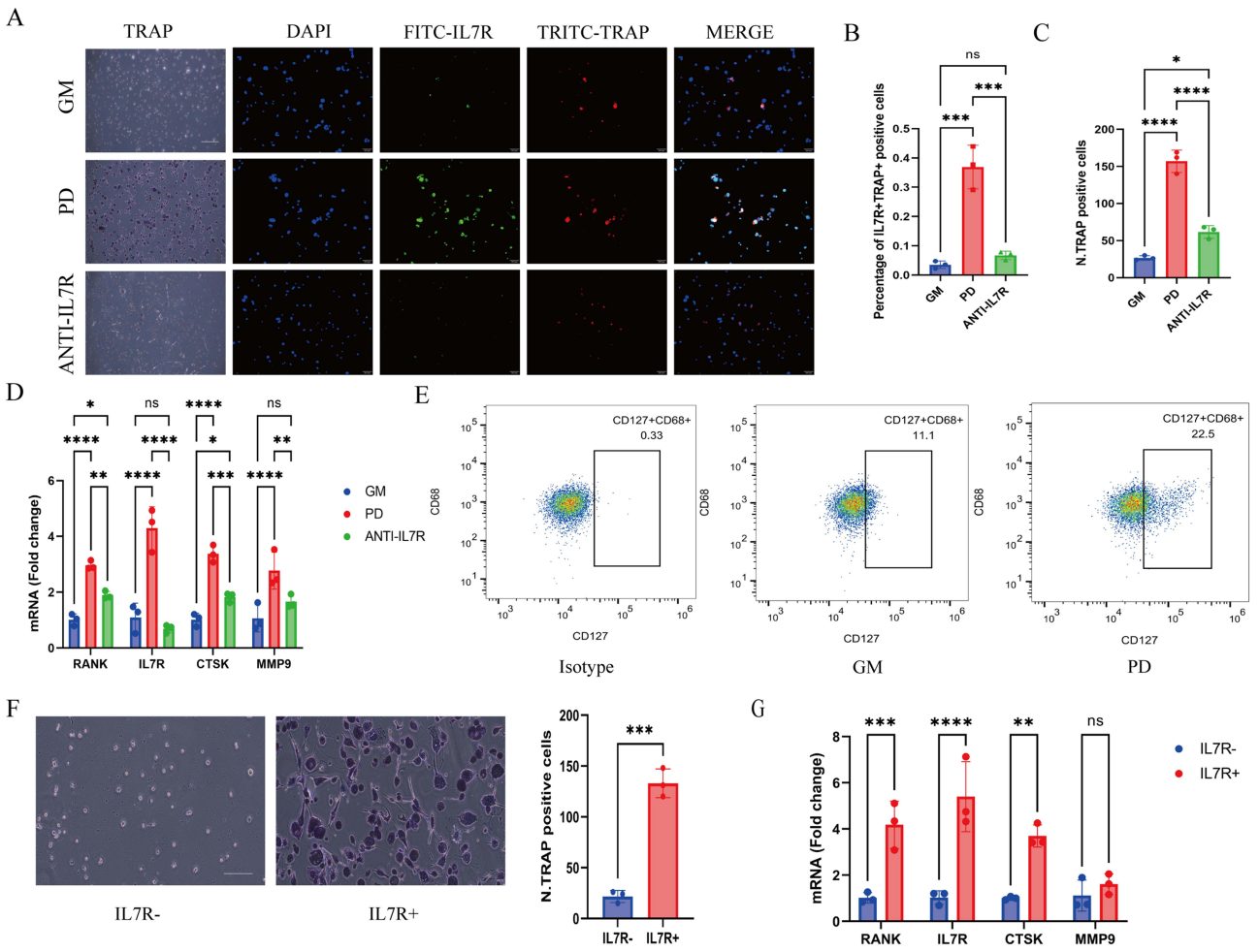

Figure 4 IL-7R+ Macrophages exhibit osteoclastic characteristics under in vitro periodontitis-stimulated condition. GM: control. PD: M0 macrophages were treated with 100ng/mL Pg.LPS for 48 hours before osteoclast induction. ANTI-IL7R: IL7R blocking antibody was added at 1μg/mL to cells during the Pg.LPS induction. (**A**) Right raw: Representative images of the immunofluorescence of TRAP+IL7R+ macrophage, n=3. (IL-7R (FITC), TRAP (TRITC), and DAPI) Left raw: Representative images of TRAP staining. (**B**) Quantitative analysis for percentage of IL7R+TRAP+ positive cells in Immunofluorescence (n=3). (**C**) Quantitative analysis for TRAP^{+} cells of GM, PD, and ANTI-IL7R groups in TRAP staining (n=3). (**D**) The mRNA expression of RANK, IL-7R, CTSK, and MMP9 in GM, PD, and ANTI-IL7R groups (n=3). (**E**) Flow Cytometric Analysis of IL7R and CD68 Expression in THP-1 Macrophages in GM and PD (n=3). (**F**) Representative images of TRAP staining of the IL7R- and the IL7R+ macrophages after treatment with M-CSF (30 ng/mL) and RANKL (50ng/mL) (n=3). (**G**) The mRNA expression of RANK, IL-7R, CTSK, and MMP9 in IL7R- and IL7R+ groups (n=3). Scale bar, 0.1 mm. One-way ANOVA with Tukey's multiple comparisons test. All data are means ± SD. *p<0.05, **p<0.01, ***p<0.001, ****p<0.0001.
Abbreviation: ns, No Significant difference.

frequency of IL7R^{+} macrophages rose in conjunction with osteoclast induction, and blocking IL7R inhibited osteoclast differentiation.

Blocking the IL7/IL7R Pathway Inhibits Osteoclast Differentiation in Mice

To elucidate the role of IL7R in periodontitis, we induced a periodontitis model in mice. As anticipated, administration of IL7R antibodies mitigated bone loss induced by ligature-mediated periodontitis (Figure 5A). The ANTI-IL7R group exhibited a significantly higher bone volume fraction (BV/TV) compared to the periodontitis group, with no discernible difference observed relative to the GM (Figure 5B). Measurement of cementoenamel junction to alveolar bone crest (CEJ-ABC) distance revealed decreased bone resorption in the ANTI-IL7R group (Figure 5C).

These findings were further corroborated by tartrate-resistant acid phosphatase (TRAP) staining, which demonstrated an increased presence of osteoclasts in proximity to the second molar within the periodontitis group (Figure 5D and E). Additionally, the panoramic stained sections further illustrate these observations and are presented in Figure S2. In the same region, co-immunostaining of IL7R with TRAP demonstrated increased expression of IL7R and TRAP in the periodontitis group relative to

https://doi.org/10.2147/JIR.S524284

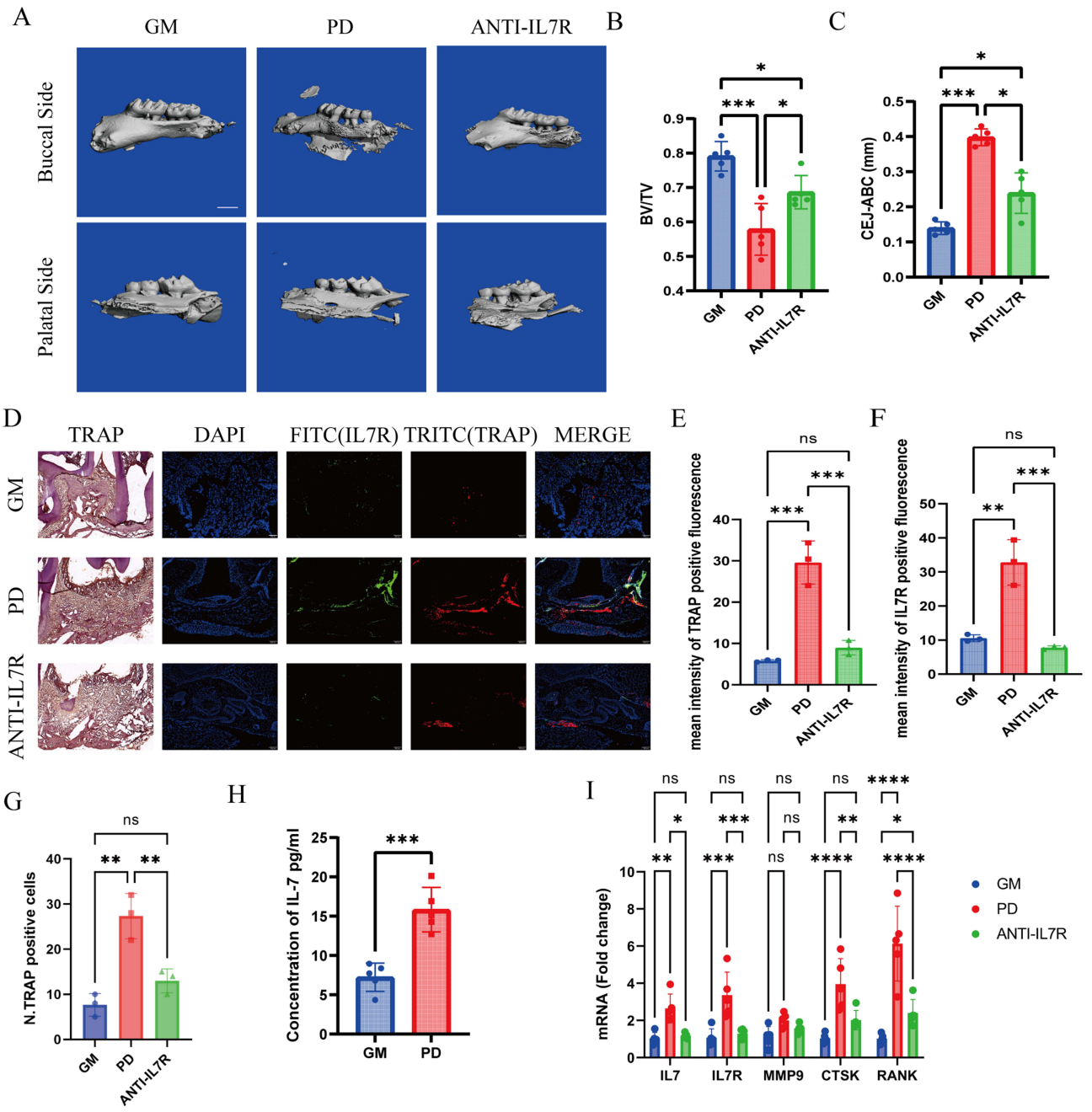

Figure 5 Blocking the IL7/IL7R pathway inhibits osteoclast in mice. GM: healthy control. PD: Ligature-induced periodontitis mice for two weeks. ANTI-IL7R: Ligature-induced periodontitis mice were gingivally injected in situ with IL7R blocking antibodies (5μg each) on days 0,3,6,9,12. (**A**) Representative three-dimensional micro-CT images of the alveolar bone of the GM (control), PD, and ANTI-IL7R mice treated with IL-7R inhibitor, n=5. One-way ANOVA with Tukey's multiple comparisons test. Scale bar, 0.1 mm. (**B** and **C**) Quantitative analysis of bone volume/tissue volume (BV/TV) and the distance from the cemento-enamel junction (CEJ) to the alveolar bone crest (ABC) based on the micro CT analysis, (n=5). (**D**) Right raw: Representative images of the immunofluorescence of $TRAP^{+}IL\text{-}7R^{+}$ macrophage, n=3. (IL-7R (FITC), TRAP (TITRC), and DAPI (blue) staining of nuclei) Left raw: TRAP staining for tissue around the second maxillary molar. Scale bar, 0.1mm. (**E**) Quantitative results of the N. TRAP-positive cells in TRAP staining, n=3. (**F** and **G**) Quantitative results of the mean intensity of $TRAP^{+}$ and $IL\text{-}7R^{+}$ fluorescence, n=3. (**H**) IL7 Concentration in GM and PD Gingival Tissues by ELISA, n=5. (**I**) The mRNA expression of IL-7R, IL-7, CTSK, and RANK in GM, PD, and ANTI-IL7R groups, n=5. One-way ANOVA with Tukey's multiple comparisons test. All data are means ± SD and are performed by one-way ANOVA with Tukey's multiple comparisons test. *p<0.05, **p<0.01, ***p<0.001, ****p<0.0001. **Abbreviation**: ns, No Significant difference.

both the GM and ANTI-IL7R group, with significant enhancement in IL7R+TRAP+ cells (Figure 5D, F, and G). These findings demonstrated the association of $IL7R^{+}$ macrophages with osteoclast activity in periodontitis. ELISA revealed significantly higher IL7 secretion in the PD group compared to the GM group (Figure 5H). RT-qPCR revealed elevated expression levels of IL7R,

IL7, and several osteoclast-related genes including RANK, MMP9, and CTSK in the periodontitis group compared to both the GM and ANTI-IL7R groups (Figure 5I).

We subsequently merged single-cell datasets from mouse studies for further analysis. After conducting independent quality control assessments of the original datasets, we analyzed IL7R expression in macrophages from the GM and PD groups, which revealed significantly elevated levels in the PD group (Figure S3). Collectively, these results demonstrate increased expression of IL7R in a murine model of periodontitis and underscore the significance of $IL7R^+$ macrophages as a subpopulation linked to osteoclastogenesis in periodontitis.

Fibroblast-Derived IL7 Induces Osteoclastic Differentiation in $IL7R^+$ Macrophages via the IL7/IL7R Axis

Previous investigations have highlighted an upregulation of IL7, the principal ligand for IL7R, in patients suffering from periodontitis.[15,22] The IL7R is exclusively activated by the cytokine IL7.[23] In our studies, clinical samples detecting IL7 concentrations in healthy and periodontitis-affected gingiva via ELISA highlighted its marked increase in periodontitis (Figure S4), with specific concentrations detailed in Supplementary Table 2. We hypothesize that IL7-IL7R interaction plays a critical role in the osteoclast differentiation process of $IL7R^+$ macrophages.

Utilizing CellChat for cell-cell communication analysis, we observed comprehensive communication in periodontitis (Figure 6A). In the global IL7/IL7R communication network, the IL7/IL7R communication strength between fibroblasts and macrophages was relatively strong (Figure 6B). To focus on specific macrophage subpopulations, we set macrophage and monocyte subgroups as receivers and other cell types as sources. As a result, the communication between $IL7R^+$ macrophage subgroups and fibroblasts was identified as the strongest (Figure 6C). Dot plots highlighting major inflammatory pathways with $IL7R^+$ macrophages as receptors showed a strong IL7/IL7R signaling interaction between fibroblasts and $IL7R^+$ macrophages (Figure 6D). The inflammation-induced markers in HGF-1 cells are IL6 and IL8, and IL7 was also detected, as assessed by ELISA and qPCR under inflammatory conditions.[24,25] The results showed a significant increase in the expression levels of these factors after Pg-LPS treatment (Figure 6E and F). Therefore, we established a co-culture system to determine whether fibroblasts stimulated by periodontal inflammation promote osteoclast differentiation in macrophages and to explore the role of the IL7/IL7R signaling pathway in this process. To investigate the role of the IL7/IL7R signaling pathway in the fibroblast–macrophage axis, we used an IL7-blocking antibody. TRAP staining results showed that the supernatant from the PD group significantly stimulated osteoclast differentiation, and the use of IL7 inhibitory antibodies partially blocked this process (Figure 6G and H). Immunofluorescence further supported this result, showing a higher proportion of TRAP+IL7R+ macrophages in the co-culture with PD group supernatant (Figure 6G and I). RT-qPCR revealed elevated expression levels of IL7R, IL7, and several osteoclast-related genes, including RANK, MMP9, and CTSK, in the periodontitis group co-culture compared to both the GM and ANTI-IL7 groups (Figure 6J).

In conclusion, our bioinformatics analysis and in vitro experiments confirmed that fibroblasts in periodontitis secrete IL7, which promotes osteoclast differentiation in $IL7R^+$ macrophages.

Discussions

Our study establishes a comprehensive cellular atlas of periodontitis by integrating scRNA-seq and bulk RNA-seq datasets across multiple cohorts, revealing previously unrecognized heterogeneity within gingival macrophages. Our approach, integrating human single-cell periodontitis data through rigorous data filtering and cleaning, led to the creation of a detailed scRNA-seq atlas of the gingival microenvironment affected by periodontitis. This atlas unveiled a subset of $IL7R^+$ macrophages pivotal in osteoclast differentiation and further analysis through the functional trajectory of $IL7R^+$ macrophages. Ultimately, we employed a variety of machine learning algorithms to predict periodontitis for the prognostication of periodontitis onset. The $IL7R^+$ macrophages' relative high expression genes have the highest prediction rates by the random forest and stepglm models. We confirmed the ratio of $IL7R^+$ macrophages and the communication of the IL7/IL7R signaling axis through in vivo and in vitro experiments. Additionally, we demonstrated that fibroblast-derived IL7 acts on $IL7R^+$ macrophages, promoting osteoclast differentiation.

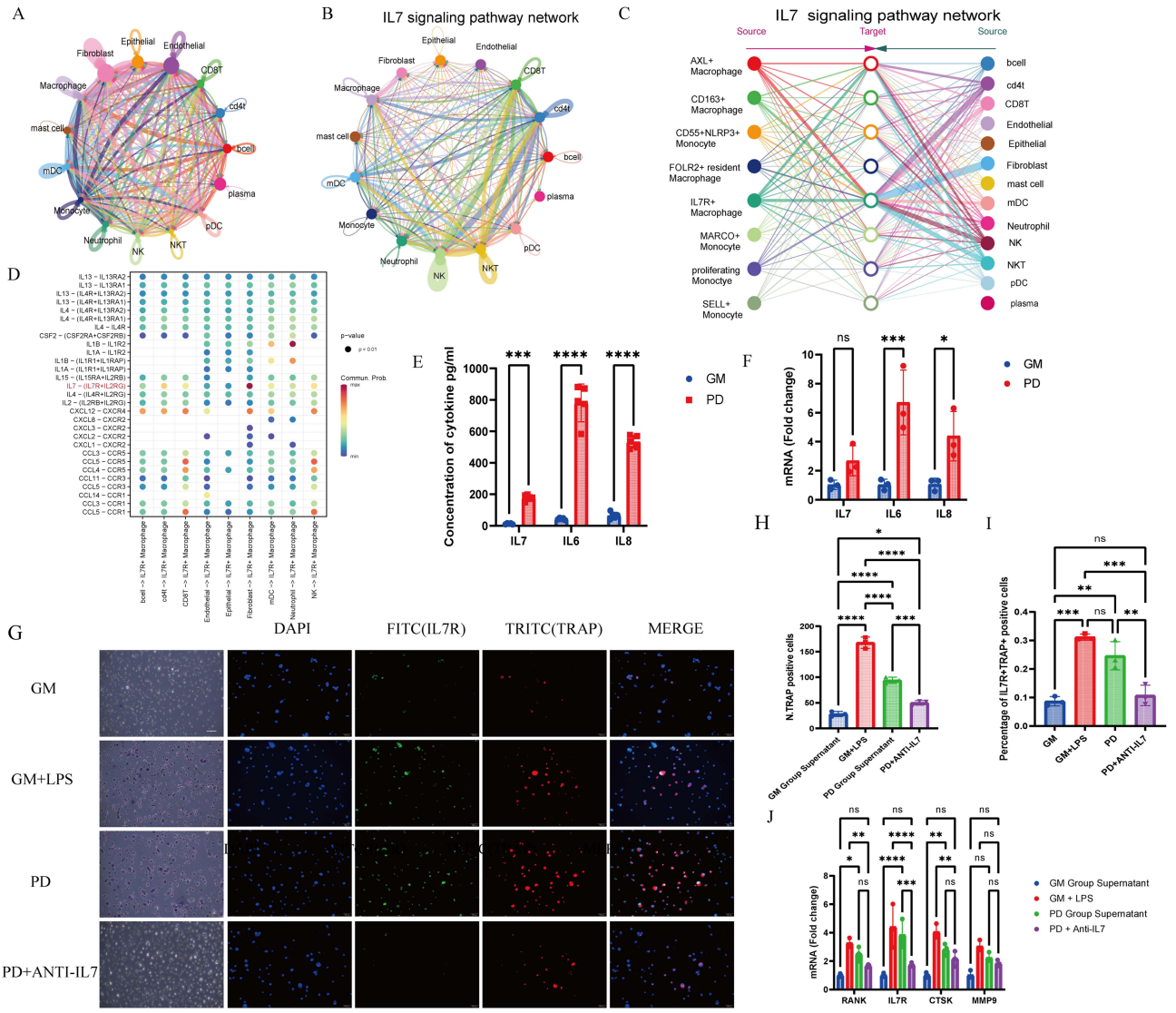

Figure 6 Fibroblast-Derived IL7 Induces Osteoclastic Differentiation in IL7R^{+} Macrophages via the IL7/IL7R Axis. (**A**) Chord chart displaying Intercellular signaling pathways weighs of major cell types in gingival microenvironment. (**B**) Chord chart displaying IL7- IL7R interaction weighs in major cell types. (**C**) Network visualization of IL7/IL7R communication strength between macrophages, monocytes, and other cell types, with macrophages and monocytes as receptors. (D)Bubble plot of ligand-receptor-mediated interactions between macrophage subtypes. The dot color and size represent the calculated communication probability and p values. (**E**) IL7, IL6, and IL8 concentrations in GM and PD HGF-1 cells measured by ELISA, n=5. GM: Blank control group cultured in medium. PD: Group cultured in medium with LPS stimulation. The supernatant was collected 1 day after stimulation. (**F**) The mRNA expression of IL7, IL6, and IL8 in HGF-1 cells, n=3. (**G**) Right raw: Representative images of the immunofluorescence of TRAP+IL-7R+ macrophage, n=3. (IL-7R (FITC), TRAP (TRITC), and DAPI) Left raw: Representative images of TRAP staining, n=3. The supernatant was collected 1 day after stimulation. GM Co-culture: THP-1 co-cultured with supernatant of HGF-1 GM groups; GM+LPS: THP-1 co-cultured with GM group supernatant added 100ng/mL LPS; PD group supernatant: THP-1 co-cultured with supernatant of HGF-1 PD groups; Co-culture PD ANTI-IL7 group: THP-1 co-cultured with PD group supernatant added 1μg/mL IL7 blocking antibody (1μg/mL). (**H**) Quantitative analysis for TRAP+ cells, n=3 (**I**) Quantitative analysis for percentage of IL7R+TRAP+ positive cells in Immunofluorescence. (**J**) The mRNA expression of IL7R, RANK, CTSK, and MMP9, in THP-1 cells after co-culture in GM, PD, and ANTI-IL7R groups (n=3). One-way ANOVA with Tukey's multiple comparisons test. *p<0.05, **p<0.01, ***p<0.001, ****p<0.0001.
Abbreviation: ns, No Significant difference.

Recently, research on single-cell sequencing and integrative studies across various regions have increasingly employed large-sample or multi-dataset integrative analyses to increase the number of samples, enhancing both the credibility and generalizability of the findings.[26–29] While previous studies in PD relied on single-cohort scRNA-seq analyses, our cross-dataset integration strategy minimized batch effects and identified conserved disease-associated signatures, a critical advance given the high technical variability in public PD datasets.[30,31] This approach aligns with recent trends in rheumatoid arthritis and osteoporosis research, where multi-omics convergence has accelerated

therapeutic target discovery.[32,33] However, unlike these fields, PD research lags in leveraging existing data resources—a gap our study begins to address.

After identifying IL-7R$^+$ macrophage as a periodontitis-specific subcluster, we found that the IL7/IL7R signaling axis also played a pathogenic role in bone resorption diseases such as arthritis and osteoporosis.[34] Particularly noteworthy is the role of IL-7 in joint inflammation of rheumatoid arthritis (RA) patients, attributed to the activation of macrophages.[35] For osteoclast differentiation, recent studies suggested that rheumatoid arthritis (RA)-naive myeloid cells were remodeled into osteoclast by IL-7 ligation, while in postmenopausal osteoporosis, IL7 from bone marrow stromal cells promotes osteoclastogenesis through similar mechanisms.[36,37] Our discovery of gingival fibroblasts as a previously unrecognized IL7 source in periodontitis reveals a tissue-specific stromal-immune crosstalk mechanism. Unlike IL7 derived from T cells in rheumatoid arthritis or bone marrow stromal cells in osteoporosis, the gingival fibroblast-orchestrated IL7 production appears uniquely shaped by local microbial challenges, suggesting a pathogen-adapted stromal response in periodontal inflammation. This finding expands the functional repertoire of fibroblasts beyond extracellular matrix remodeling, positioning them as active immune modulators that bridge microbial sensing and osteoclast activation.

The identification of fibroblast-derived IL7 as a microbial sensor-osteoclast activation bridge offers a spatially precise therapeutic avenue for periodontitis. Blocking IL7/IL7R signaling could locally dampen osteolysis while preserving systemic bone turnover, an advantage over conventional anti-resorptive drugs. In clinical trials, IL-7 antagonists have been extensively evaluated.[21] For instance, Pfizer's PF-06342674 (RN168) has completed a Phase I trial in patients with type 1 diabetes and multiple sclerosis,[38] while OSE's anti–IL-7Rα monoclonal antibody (OSE-127) is currently undergoing a Phase I trial in healthy volunteers, with plans for subsequent Phase II evaluations in patients with inflammatory bowel disease and Sjögren's syndrome.[39] However, their primary therapeutic mechanism is the inhibition of IL-7–mediated T cell differentiation, and their application to suppress macrophage-derived osteoclast differentiation has not yet been explored. Topical administration using hydrogel carriers or nanoparticle-encapsulated anti–IL7/IL7R antibodies may confine drug activity to periodontal pockets by exploiting the anatomical accessibility of gingival tissues.[40] This strategy echoes successful intra-articular IL7R blockade in rheumatoid arthritis models, which reduced bone erosion without affecting systemic lymphocytes. Nonetheless, IL7's role in lymphoid homeostasis necessitates patient stratification through IL7 biomarker profiling and real-time adaptive immunity monitoring.[41] Moreover, the fibroblast-centric mechanism advocates for stromal cell-targeted delivery systems to improve therapeutic precision. Although current IL7/IL7R inhibitors are promising translational candidates, their efficacy in periodontal models and optimal delivery methods require further validation.

Our findings both align with and extend prior knowledge on IL7/IL7R signaling in bone biology. Earlier studies reported conflicting roles of IL7 in osteoclastogenesis: systemic IL7 administration was shown to inhibit bone resorption in osteoporosis models by suppressing T cell-derived RANKL,[36] whereas myeloid-specific IL7R activation promoted osteoclast differentiation via STAT5-dependent metabolic reprogramming.[42,43] This discrepancy suggests cell type- and context-dependent effects of IL7. In periodontitis, we demonstrate that fibroblast-derived IL7—rather than lymphoid or circulating IL7—acts locally on IL7R$^+$ macrophages to license their osteoclastogenic capacity. This spatial specificity may explain why IL7 exhibits pro-osteoclastic effects here, contrasting its anti-resorptive role in osteoporosis.[44,45] Furthermore, our experimental data revealed that IL7R$^+$ macrophages co-express both IL7R and RANK, enabling synergistic activation of STAT5 and NF-κB pathways, a mechanism not previously described in other IL7-related bone disorders.

A critical unanswered question is how periodontal pathogens reprogram fibroblasts to overexpress IL7. Emerging evidence suggests that pathogens like Porphyromonas gingivalis may directly modulate fibroblast cytokine production through protease-activated receptors (PARs) or epigenetic remodeling.[46] For instance, P. gingivalis LPS induces metabolic and epigenetic reprogramming in gingival fibroblasts via the PI3K/AKT pathway, enhancing pro-inflammatory cytokine secretion.[47,48] Furthermore, the polymicrobial synergy between P. gingivalis and commensal bacteria (eg, Streptococcus gordonii) may amplify IL7 expression through cross-kingdom signaling, as observed in studies where co-culture with oral pathogens altered fibroblast inflammatory responses.[49,50] Future studies should delineate whether pathogen-associated molecular patterns (PAMPs) or metabolite exchanges (eg, succinate) underlie this phenomenon. Spatially resolved single-cell technologies will be essential to map IL7R$^+$ macrophage-fibroblast interaction niches—particularly in deep periodontal pockets where anaerobic pathogens thrive.[51] Additionally, single-cell chromatin accessibility profiling (scATAC-seq) could identify transcription factors (eg, IRF4, STAT3) governing IL7 upregulation in

pathogen-exposed fibroblasts, as epigenetic dysregulation (eg, histone methylation) has been implicated in fibroblast activation during periodontitis.[52]

Although the IL7/IL7R signaling pathway has been demonstrated as one of the pathogenic mechanisms underlying periodontitis through in vivo and in vitro experiments, clinical samples, and single-cell analyses, interpatient variability remains uncertain. This uncertainty necessitates the investigation of larger clinical cohorts and the conduct of additional experiments to validate these findings. Although our study concentrated on the IL7/IL7R axis as the predominant pathway, alternative mechanisms of osteoclast differentiation may coexist for chronic periodontitis.[53,54] For instance, proinflammatory cytokines such as TNF-α and IL-1β, which are highly expressed in periodontal lesions, can directly trigger NF-κB signaling in osteoclast precursors independent of RANKL.[55,56] Similarly, components of the complement system (eg, C5a) and alarmins (such as S100A8/A9) have been shown to facilitate osteoclastogenesis via non-canonical pathways.[57,58] The potential interplay between IL7R signaling and these alternative routes remains to be elucidated, particularly in patients who exhibit suboptimal responses to IL7R-targeted therapies.

Taken together, our study has shed light on the intricate mechanisms underlying periodontitis, offering valuable insights into potential therapeutic targets and predictive models for their treatment. By elucidating these mechanisms, we have paved the way for developing innovative research patterns that can revolutionize the management and treatment of periodontitis.

Conclusions

In summary, we identified $IL7R^+$ macrophages as potential precursor cells for osteoclast differentiation in periodontitis through bioinformatics analyses and in vitro/in vivo verification. Crucially, gingival fibroblasts were revealed as the predominant IL7 source that activates $IL7R^+$ macrophages through the IL7/IL7R signaling pathway to drive pathological osteoclastogenesis. Therapeutically, blockade of either stromal-derived IL7 production or its receptor signaling effectively suppressed periodontitis-related bone resorption. These results reveal a novel mechanism contributing to the chronic nature of periodontitis and underscore the pathway's potential as a promising therapeutic target for controlling periodontal bone loss.

Data Available Statement

The data that support the findings of this study are available from the corresponding author upon reasonable request.

Acknowledgments

This research was funded by the National Natural Science Foundation of China (U22A20316, 82001109), Guangdong Basic and Applied Basic Research Foundation (2023A1515010205), Science and Technology Program of Guangzhou (2024A04J4852).

Author Contributions

All authors made a significant contribution to the work reported, whether that is in the conception, study design, execution, acquisition of data, analysis and interpretation, or in all these areas; took part in drafting, revising or critically reviewing the article; gave final approval of the version to be published; have agreed on the journal to which the article has been submitted; and agree to be accountable for all aspects of the work.

Disclosure

The authors declare no competing interests for this work.

References

1. Germen M, Baser U, Lacin CC, et al. Periodontitis prevalence, severity, and risk factors: a comparison of the AAP/CDC case definition and the EFP/AAP classification. *Int J Environ Res Public Health*. 2021;18(7):3459. doi:10.3390/ijerph18073459
2. Amaral AL, Lund B, Andrade SA. Would it really be necessary to use metronidazole as an adjunct in the surgical treatment of periodontitis? *Evid Based Dent*. 2024;25(4):180–181. doi:10.1038/s41432-024-01027-1
3. Tossetta G, Fantone S, Togni L, et al. Modulation of NRF2/KEAP1 signaling by phytotherapeutics in periodontitis. *Antioxidants*. 2024;13(10):1270. doi:10.3390/antiox13101270

4. Slots J. Periodontitis: facts, fallacies and the future. *Periodontol*. 2017;75(1):7–23.
5. Zhang X, Hu Z, Zhu X, et al. Treating periodontitis-a systematic review and meta-analysis comparing ultrasonic and manual subgingival scaling at different probing pocket depths. *BMC Oral Health*. 2020;20(1):176. doi:10.1186/s12903-020-01117-3
6. Deas DE, Moritz AJ, Sagun RS, et al. Scaling and root planing vs conservative surgery in the treatment of chronic periodontitis. *Periodontol*. 2016;71(1):128–139. doi:10.1111/prd.12114
7. Zhou M, Graves DT. Impact of the host response and osteoblast lineage cells on periodontal disease. *Front Immunol*. 2022;13:998244. doi:10.3389/fimmu.2022.998244
8. Yang J, Zhu Y, Duan D, et al. Enhanced activity of macrophage M1/M2 phenotypes in periodontitis. *Arch Oral Biol*. 2018;96:234–242. doi:10.1016/j.archoralbio.2017.03.006
9. Locati M, Curtale G, Mantovani A. Diversity, mechanisms, and significance of macrophage plasticity. *Annu Rev Pathol*. 2020;15:123–147. doi:10.1146/annurev-pathmechdis-012418-012718
10. Murray PJ, Allen J, Biswas S, et al. Macrophage activation and polarization: nomenclature and experimental guidelines. *Immunity*. 2014;41(1):14–20. doi:10.1016/j.immuni.2014.06.008
11. Sun X, Gao J, Meng X, et al. Polarized macrophages in periodontitis: characteristics, function, and molecular signaling. *Front Immunol*. 2021;12:763334. doi:10.3389/fimmu.2021.763334
12. Jeon HH, Huang X, Rojas Cortez L, et al. Inflammation and mechanical force-induced bone remodeling. *Periodontol*. 2024.
13. Wänman M, Betnér S, Esberg A, et al. The PerioGene North study uncovers serum proteins related to periodontitis. *J Dent Res*. 2024;103(10):999–1007. doi:10.1177/00220345241263320
14. Yu XY, Zhang Z-Q, Huang J-C, et al. IL-7-treated periodontal ligament cells regulate local immune homeostasis by modulating Treg/Th17 cell polarization. *Front Med*. 2022;9:754341. doi:10.3389/fmed.2022.754341
15. Tymkiw KD, Thunell DH, Johnson GK, et al. Influence of smoking on gingival crevicular fluid cytokines in severe chronic periodontitis. *J Clin Periodontol*. 2011;38(3):219–228. doi:10.1111/j.1600-051X.2010.01684.x
16. Xu H, Cai L, Li Z, et al. Dual effect of IL-7/IL-7R signalling on the osteoimmunological system: a potential therapeutic target for rheumatoid arthritis. *Immunology*. 2021;164(1):161–172. doi:10.1111/imm.13351
17. Zhang R, Peng S, Zhu G. The role of secreted osteoclastogenic factor of activated T cells in bone remodeling. *Jpn Dent Sci Rev*. 2022;58:227–232. doi:10.1016/j.jdsr.2022.07.001
18. Chen Y, Wang H, Yang Q, et al. Single-cell RNA landscape of the osteoimmunology microenvironment in periodontitis. *Theranostics*. 2022;12(3):1074–1096. doi:10.7150/thno.65694
19. Agrafioti P, Morin-Baxter J, Tanagala KKK, et al. Decoding the role of macrophages in periodontitis and type 2 diabetes using single-cell RNA-sequencing. *FASEB J*. 2022;36(2):e22136. doi:10.1096/fj.202101198R
20. Lazarov T, Juarez-Carreño S, Cox N, et al. Physiology and diseases of tissue-resident macrophages. *Nature*. 2023;618(7966):698–707. doi:10.1038/s41586-023-06002-x
21. Barata JT, Durum SK, Seddon B. Flip the coin: IL-7 and IL-7R in health and disease. *Nat Immunol*. 2019;20(12):1584–1593. doi:10.1038/s41590-019-0479-x
22. Schulz S, Immel UD, Just L, et al. Epigenetic characteristics in inflammatory candidate genes in aggressive periodontitis. *Hum Immunol*. 2016;77(1):71–75. doi:10.1016/j.humimm.2015.10.007
23. Wang C, Kong L, Kim S, et al. The role of IL-7 and IL-7R in cancer pathophysiology and immunotherapy. *Int J mol Sci*. 2022;23(18).
24. Wenjing S, Mengmeng L, Lingling S, et al. Galectin-3 inhibition alleviated LPS-induced periodontal inflammation in gingival fibroblasts and experimental periodontitis mice. *Clin Sci*. 2024;138(12):725–739. doi:10.1042/CS20240036
25. Baldeón Rojas L, Weigelt K, de Wit H, et al. Study on inflammation-related genes and microRNAs, with special emphasis on the vascular repair factor HGF and miR-574-3p, in monocytes and serum of patients with T2D. *Diabetol Metab Syndr*. 2016;8:6. doi:10.1186/s13098-015-0113-5
26. Hu J, Wang S-G, Hou Y, et al. Multi-omic profiling of clear cell renal cell carcinoma identifies metabolic reprogramming associated with disease progression. *Nat Genet*. 2024;56(3):442–457. doi:10.1038/s41588-024-01662-5
27. Chu Y, Dai E, Li Y, et al. Pan-cancer T cell atlas links a cellular stress response state to immunotherapy resistance. *Nat Med*. 2023;29(6):1550–1562. doi:10.1038/s41591-023-02371-y
28. Salcher S, Sturm G, Horvath L, et al. High-resolution single-cell atlas reveals diversity and plasticity of tissue-resident neutrophils in non-small cell lung cancer. *Cancer Cell*. 2022;40(12):1503–1520.e8. doi:10.1016/j.ccell.2022.10.008
29. De Donno C, Hediyeh-Zadeh S, Moinfar AA, et al. Population-level integration of single-cell datasets enables multi-scale analysis across samples. *Nat Methods*. 2023;20(11):1683–1692. doi:10.1038/s41592-023-02035-2
30. Yan M, Tsukasaki M, Muro R, et al. Identification of an intronic enhancer regulating RANKL expression in osteocytic cells. *Bone Res*. 2023;11(1):43. doi:10.1038/s41413-023-00277-6
31. Wu Y, Ma J, Yang X, et al. Neutrophil profiling illuminates anti-tumor antigen-presenting potency. *Cell*. 2024;187(6):1422–1439.e24. doi:10.1016/j.cell.2024.02.005
32. Zhang F, Wei K, Slowikowski K, et al. Defining inflammatory cell states in rheumatoid arthritis joint synovial tissues by integrating single-cell transcriptomics and mass cytometry. *Nat Immunol*. 2019;20(7):928–942. doi:10.1038/s41590-019-0378-1
33. Wu S, Ohba S, Matsushita Y. Single-cell RNA-sequencing reveals the skeletal cellular dynamics in bone repair and osteoporosis. *Int J mol Sci*. 2023;24(12).
34. Zhao JJ, Wu Z-F, Yu Y-H, et al. Effects of interleukin-7/interleukin-7 receptor on RANKL-mediated osteoclast differentiation and ovariectomy-induced bone loss by regulating c-Fos/c-Jun pathway. *J Cell Physiol*. 2018;233(9):7182–7194. doi:10.1002/jcp.26548
35. Pickens SR, Chamberlain ND, Volin MV, et al. Characterization of interleukin-7 and interleukin-7 receptor in the pathogenesis of rheumatoid arthritis. *Arthritis Rheum*. 2011;63(10):2884–2893. doi:10.1002/art.30493
36. Meyer A, Parmar PJ, Shahrara S. Significance of IL-7 and IL-7R in RA and autoimmunity. *Autoimmun Rev*. 2022;21(7):103120. doi:10.1016/j.autrev.2022.103120
37. Kim SJ, Chang HJ, Volin MV, et al. Macrophages are the primary effector cells in IL-7-induced arthritis. *Cell mol Immunol*. 2020;17(7):728–740. doi:10.1038/s41423-019-0235-z

38. Williams JH, Udata C, Ganguly BJ, et al. Model-based characterization of the pharmacokinetics, target engagement biomarkers, and immunomodulatory activity of PF-06342674, a humanized mAb against IL-7 receptor-α, in adults with type 1 diabetes. *Aaps J*. 2020;22(2):23. doi:10.1208/s12248-019-0401-3
39. Poirier N, Baccelli I, Belarif L, et al. First-in-human study in healthy subjects with the noncytotoxic monoclonal antibody OSE-127, a strict antagonist of IL-7Rα. *J Immunol*. 2023;210(6):753–763. doi:10.4049/jimmunol.2200635
40. Pan Q, Zong Z, Li H, et al. Hydrogel design and applications for periodontitis therapy: a review. *Int J Biol Macromol*. 2025;284(Pt 1):137893. doi:10.1016/j.ijbiomac.2024.137893
41. Park JH, Waickman AT, Reynolds J, et al. IL7 receptor signaling in T cells: a mathematical modeling perspective. *Wiley Interdiscip Rev Syst Biol Med*. 2019;11(5):e1447. doi:10.1002/wsbm.1447
42. Winer H, Rodrigues GOL, Hixon JA, et al. IL-7: comprehensive review. *Cytokine*. 2022;160:156049. doi:10.1016/j.cyto.2022.156049
43. Zhang B, Zhang Y, Xiong L, et al. CD127 imprints functional heterogeneity to diversify monocyte responses in inflammatory diseases. *J Exp Med*. 2022;219(2). doi:10.1084/jem.20211191
44. Frase D, Lee C, Nachiappan C, et al. The inflammatory contribution of B-lymphocytes and neutrophils in progression to osteoporosis. *Cells*. 2023;12(13):1744. doi:10.3390/cells12131744
45. Weitzmann MN, Pacifici R. Estrogen regulation of immune cell bone interactions. *Ann N Y Acad Sci*. 2006;1068:256–274. doi:10.1196/annals.1346.030
46. Martin CR, Osadchiy V, Kalani A, et al. The brain-gut-microbiome axis. *Cell Mol Gastroenterol Hepatol*. 2018;6(2):133–148. doi:10.1016/j.jcmgh.2018.04.003
47. Guo X, Huang Z, Ge Q, et al. Glipizide Alleviates Periodontitis Pathogenicity via Inhibition of Angiogenesis, Osteoclastogenesis and M1/M2 Macrophage Ratio in Periodontal Tissue. *Inflammation*. 2023;46(5):1917–1931. doi:10.1007/s10753-023-01850-1
48. Liu J, Tian H, Ju J, et al. Porphyromonas gingivalis -lipopolysaccharide induced gingival fibroblasts trained immunity sustains inflammation in periodontitis. *J Periodontal Res*. 2024. doi:10.1111/jre.13372
49. Zhao JJ, Feng X-P, Zhang X-L, et al. Effect of Porphyromonas gingivalis and Lactobacillus acidophilus on secretion of IL1B, IL6, and IL8 by gingival epithelial cells. *Inflammation*. 2012;35(4):1330–1337. doi:10.1007/s10753-012-9446-5
50. Su W, Shi J, Zhao Y, et al. Gingival fibroblasts dynamically reprogram cellular metabolism during infection of Porphyromonas gingivalis. *Arch Oral Biol*. 2021;121:104963. doi:10.1016/j.archoralbio.2020.104963
51. Huang Y, Tang Y, Zhang R, et al. Role of periodontal ligament fibroblasts in periodontitis: pathological mechanisms and therapeutic potential. *J Transl Med*. 2024;22(1):1136. doi:10.1186/s12967-024-05944-8
52. Jurdziński KT, Potempa J, Grabiec AM. Epigenetic regulation of inflammation in periodontitis: cellular mechanisms and therapeutic potential. *Clin Clin Epigenet*. 2020;12(1):186. doi:10.1186/s13148-020-00982-7
53. Jang JS, Hong SJ, Mo S, et al. PINK1 restrains periodontitis-induced bone loss by preventing osteoclast mitophagy impairment. *Redox Biol*. 2024;69:103023. doi:10.1016/j.redox.2023.103023
54. Hascoët E, Blanchard F, Blin-Wakkach C, et al. New insights into inflammatory osteoclast precursors as therapeutic targets for rheumatoid arthritis and periodontitis. *Bone Res*. 2023;11(1):26. doi:10.1038/s41413-023-00257-w
55. Theill LE, Boyle WJ, Penninger JM. RANK-L and RANK: t cells, bone loss, and mammalian evolution. *Annu Rev Immunol*. 2002;20:795–823. doi:10.1146/annurev.immunol.20.100301.064753
56. Xu J, Wu HF, Ang ESM, et al. NF-kappaB modulators in osteolytic bone diseases. *Cytokine Growth Factor Rev*. 2009;20(1):7–17. doi:10.1016/j.cytogfr.2008.11.007
57. Pimenta-Lopes C, Sánchez-de-diego C, Deber A, et al. Inhibition of C5AR1 impairs osteoclast mobilization and prevents bone loss. *Mol Ther*. 2023;31(8):2507–2523. doi:10.1016/j.ymthe.2023.04.022
58. Di Ceglie I, Kruisbergen NNL, van den Bosch MHJ, et al. Fc-gamma receptors and S100A8/A9 cause bone erosion during rheumatoid arthritis. Do they act as partners in crime? *Rheumatology*. 2019;58(8):1331–1343. doi:10.1093/rheumatology/kez218